A SUPERCONDUCTING FUSION TRANSMUTATION OF WASTE REACTOR

A Thesis

Presented to

The Academic Faculty

By

Andrew N. Mauer

In Partial Fulfillment

of the Requirements for the Degree

Master of Science in Nuclear Engineering

Woodruff School of Mechanical Engineering

Georgia Institute of Technology

August 2002

A Superconducting Fusion Transmutation of Waste Reactor

Approved by:

Dr. Weston Stacey Jr., Advisor

Dr. John Mandrekas

Dr. C.K. Chris Wang

Date Approved 8/12/02

ACKNOWLEDGEMENT

I am forever indebted to Dr. Weston Stacey Jr., my advisor, who has given me assistance and direction with the development and research of this thesis. His voluminous knowledge, experience, patience and guidance warrant my deepest gratitude.

I am humbled by the efforts expended by Dr. John Mandrekas in contributing his attention, time and guidance during the drafting of this thesis. His input was an invaluable contribution.

This paper could not have been successfully completed without the knowledge and invaluable assistance garnered from Dr. Ed Hoffman in the areas of neutronics and shielding analyses.

Finally, my mother, Mindy Mauer, has been the principal guiding light and inspiration in my life. Her encouragement and support pulled me through the days when I felt overwhelmed. Her unwillingness to give up or give in and her ambition for me to set goals and to strive toward them will always encourage me to go beyond the limits.

TABLE OF CONTENTS

LIST OF TABLES

LIST OF FIGURES

SUMMARY

A concept for a subcritical nuclear reactor driven by a tokamak fusion neutron source for the transmutation of spent nuclear fuel has recently been developed. In order to minimize the size, normal copper magnets were used, but this resulted in very large levels of ohmic heating. The purpose of this thesis is to investigate the use of superconducting magnets in the neutron source for such a transmutation reactor. A major issue is the optimization of a shield for reducing nuclear heating and radiation damage of the superconducting magnets to acceptable levels while minimizing the increase in size. Another issue is the effect of the change in size on the plasma performance of the transmutation reactor and the need for compensating changes in other plasma operating parameters.

The transmutation reactor nuclear design and the nuclear fuel cycle were not changed. In order to avoid the necessity of repeating the fuel cycle analysis, the power density, hence the transmutation rate per unit volume, was fixed at the same value as in the fusion transmutation of waste reactor (FTWR). This allows many of the power and performance related parameters for the superconducting fusion transmutation of waste reactor (FTWR-SC) to be scaled from those of the FTWR. The overall performance parameters and characteristics of the entire system are re-evaluated.

CHAPTER I. INTRODUCTION

There is substantial worldwide R&D activity devoted to the transmutation of spent nuclear fuel [1-3]. The objective of this activity is to technically evaluate the possibility of reducing the requirements for long term geological repositories for the storage of high-level radioactive waste from spent nuclear fuel (SNF) by neutron fission of the plutonium and higher actinides remaining in the spent fuel discharged from fission power reactors. Repeated recycling of this spent fuel in commercial thermal spectrum fission power reactors would not significantly reduce the repository requirements, because the destruction of actinides by fission would be offset by the production of actinides by neutron capture in ^{238}U [1,2]. Repeated recycling of the spent fuel in special purpose fast spectrum reactors could reduce the radiotoxicity of the spent nuclear fuel by a factor of about 100, limited by safety and criticality constraints [1]. These constraints could be relaxed if the reactors (fast or thermal spectrum) could be operated sub-critical, which would require a neutron source. There is a general consensus that significantly higher levels of actinide destruction can be achieved by repeated recycling of spent fuel in sub-critical reactors with a neutron source. An accelerator-spallation neutron source has been extensively studied for this application [1-6].

D-T fusion neutron sources could also be used to drive sub-critical reactors for the destruction of actinides, and a few scoping studies [7-13] have been carried out. In particular, reference 13 reviewed the requirements for a neutron source vis-à-vis the present tokamak database and found that the physics parameters routinely achieved in operating tokamaks ($H \approx 1$, β_N = 2-3) and operation at Q_p as low as 1.5-2.0 would be sufficient for a tokamak neutron source with major radius R = 3-5 m to produce

transmutation rates of hundreds to thousands of kg/FPY (full-power-year) of SNF in a sub-critical transmutation reactor.

A concept for a fusion transmutation waste reactor (FTWR) is being developed at the Georgia Institute of Technology. An initial design concept of FTWR has been developed and published [14]. Detailed nuclear design and nuclear fuel cycle analyses have been performed [15-17].

The purposes of this thesis are to identify how the physical and performance characteristics of a FTWR will be changed by the use of superconducting magnets instead of normal magnets. The general design objectives for this Superconducting Fusion Transmutation of Waste Reactor (FTWR-SC) are the same as those of FTWR, namely that it: 1) destroy the transuranic content of hundreds of metric tonnes/FPY of spent nuclear fuel; 2) utilize nuclear and processing technologies that either exist or are under development; 3) operate at a neutron multiplication factor $k_{eff} \leq 0.95$ to enhance safety; 4) be based on the existing tokamak plasma and fusion technology databases to the maximum extent possible; and 5) be self-sufficient in tritium production. In addition, the FTWR-SC produces net electric power.

CHAPTER II. FTWR DESIGN SUMMARY

We first review the design of the normal conducting magnet FTWR [14], which is the starting point for this thesis. The FTWR was designed with normal magnets in order to keep the overall size of the device at a minimum. Utilizing Oxygen Free High Conductivity (OFHC) Copper magnets resulted in a combined radial thickness of the

central solenoidal (CS) coil and the toroidal field (TF) coil of 0.57 m. In addition, the shield thickness of FTWR is 0.40 m. The radial build of FTWR is illustrated in figure 1 and the materials composition of FTWR is given in table 1.

Table 1: Materials Composition of FTWR

Component	Material
Reactor	
Fuel	Zr-transuranic alloy in Zr matrix
Clad & Structure	HT-9-like steel
Coolant	Li17Pb83 (^{6}Li enrich 20%)
Reflector	HT-9, Li17Pb83
Shield	HT-9, Li17Pb83, B_4C
Magnets	
Conductor	OFHC
Coolant	LN2
Structure	Steel
First-Wall & Divertor	
Structure	HT-9-like steel
Coolant	Li17Pb83

Midplane Radial Build

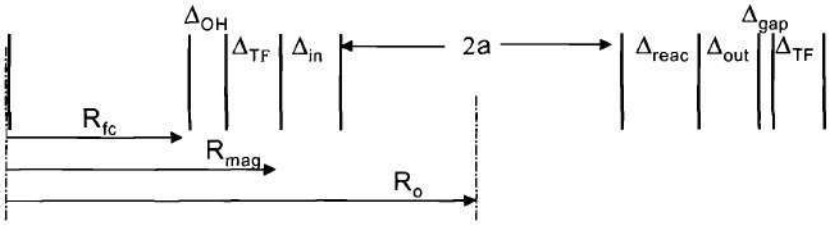

R_{fc}	=	flux core radius	=	1.24 m
Δ_{OH}	=	OH solenoid Δ	=	0.18
Δ_{TF}	=	TF coil Δ	=	0.39
Δ_{in}	=	inner refl/shld	=	0.40
a	=	minor radius	=	0.89
Δ_{reac}	=	reactor	=	0.40
Δ_{out}	=	outer refl/shld	=	0.30
Δ_{gap}	=	outer gap	=	tbd
R_o	=	major radius	=	3.10
R_{mag}	=	magnet radius	=	1.81

Note: refl/shld includes first wall, reflector, shield, and vacuum vessel

Figure 1: Radial Build of FTWR

The plasma parameters of the neutron source are for the most part routinely achieved in operating tokamaks and are given in table 2.

Table 2: Neutron Source Parameters

Parameter	Value
Plasma	
Major radius, R_0 (m)	3.1
Minor radius, a (m)	0.9
Elongation, κ	1.7
Magnetic field, B_0 (T)	6.1
Plasma current, I_p (MA)	7.0
Bootstrap current fraction	0.38
Normalized beta, β_N (%)	2.5
Confinement factor, H ITER IPB98(y,2)	1.1
Fusion power (MWth)	150
Plasma energy amplification, Q_p	2.0
Pulse length	steady-state
Magnets	
Toroidal field @ coil (T)	10.45
Central solenoid field @ coil (T)	8.0
Inductive flux (V-s)	90
Operating temperature in magnets (K)	80-100

Table 2 (continued)

Power dissipation & refrigeration (MWe)	972
Lifetime radiation dose (rads)	1.5×10^{12}
Lifetime fast neutron dose (n/cm^2)	1.8×10^{22}
First-Wall	
14 MeV neutron wall load (MW/m^2)	0.79
Surface heat load (MW/m^2)	0.34
Radiation damage (dpa/623 d cycle)	21
Tritium Inventory	
Beginning of cycle (g)	120
Maximum (g)	1000

The transmutation reactor parameters are given in table 3. The design is an adaptation of the Argonne National Laboratory (ANL) design of a transmutation reactor for an accelerator neutron source [18].

Table 3: FTWR Transmutation Reactor Parameters

Parameter	Value
Maximum multiplication constant, k_{eff}	0.95
Actinide loading (MT)	27
Maximum actinide enrichment (V/O)	45
# Hexagonal fuel assemblies	470
Fuel assembly pitch (cm)	16.1
Fuel assembly length (cm)	228
Fuel pin diameter (cm)	0.635
Average power density (kW/liter)	124
Fuel cycle	4 batch
Clad irradiation @ discharge (dpa)	150
Coolant Tin/Tout (K)	548/848
Coolant flow velocity (m/s)	0.76
Coolant mass flow rate (kg/s)	51630
Coolant pumping power (MWe)	131

The major performance parameters of FTWR are given in table 4.

Table 4: Major Performance Parameters of FTWR

Parameter	Value
Total Power (MWth)	3000
Thermal-to-electrical conversion (%)	40
Fusion Neutron Source Strength (#/s)	5.32×10^{19}
SNF Transmutation Rate (MTU/FPY)	102
Transuranic Mass Reduction in SNF (%)	99.4
Support Ratio (GWe LWR/FTWR)	3
Electrical Power Amplification, Q_e	≥ 1
Lifetime (FPY)	40
Availability (%)	60

CHAPTER III. CONCEPTUAL DESIGN & ANALYSIS OF FTWR-SC

III.A Motivation For The FTWR-SC

The primary FTWR design objective was to minimize the overall size of the reactor. Therefore, regular conducting OFHC magnets were selected in the initial FTWR design. However, at the conclusion of the design it became apparent that the ohmic heating losses associated with these magnets were too large. Therefore superconducting magnets are now being investigated to avoid these ohmic heating problems. The revised

objective is to minimize the overall size of the reactor while employing superconducting magnets and while satisfying all other physics requirements and remaining within the current physics database.

The principal motivation for this thesis is the large amount of power dissipated in ohmic heating and the large amount of power required to remove the heat from the OFHC magnets of the FTWR. The considerable ohmic heating losses associated with the OFHC magnets are also no longer a crucial design consideration when dealing with superconducting magnets.

III.B Changes Elicited By Superconducting Magnets

It is especially important that we maintain relatively the same values of the plasma density and temperature, thus we can sustain the same fusion power density. The FTWR-SC will have a 50% larger fusion power then the FTWR. As a result of increasing the radial build to accommodate the superconducting magnets the major plasma radius increased by 50%. The superconducting magnets also require that we increase the shield thickness to protect them from radiation damage. The plasma parameters also change with an alteration of the radial build. At the same time we elected to keep the same transmutation reactor design, so as a result of a 50% larger plasma and reactor volume, the fission power, tritium inventory, transuranic loading, coolant mass flow, and many other parameters all are scaled by 50%. The size of the transmutation reactor and the transmutation fuel cycle remain the same for both devices. The nuclear design remains the same as that of FTWR, with the exception of the volume and the nuclear fuel cycle. The main difference between FTWR and FTWR-SC here is

that the superconducting device is 50% larger and produces 50% more power then FTWR.

Superconducting magnets require a different coolant than regular conducting magnets and operate at different temperatures. Therefore, the magnet coolant of liquid nitrogen employed in FTWR has changed in FTWR-SC to supercritical helium. The joule heating and refrigeration power for the liquid Nitrogen coolant of FTWR was a major electrical power requirement, which no longer constitutes a major design issue of the FTWR-SC.

III.C Magnets

A tokamak fusion neutron source requires several sets of magnets. A toroidal magnet system produces the toroidal magnetic field (TF) needed to stabilize the plasma, while a central solenoid (CS) and a set of poloidal ring coils (PF) provide the changing magnetic flux (Volt-seconds) to drive the inductive plasma current and provide the equilibrium field for plasma position control and shaping.

We have focused our attention on the TF and CS systems, in this initial analysis, since they are the ones that affect the size of the FTWR-SC and can have a major impact on the recirculating power fraction of the plant.

The magnet design parameters of the ITER-FEAT design [19,20] were adapted for the new FTWR-SC design concept. The central solenoid (CS) has a flux core of 1.1 m, a radial thickness of 0.77 m and a maximum field of 13.5 T. The (18) toroidal field coils have a radial thickness of 0.91 m, a bore of 3.8 m and a maximum field of 11.8 T. The superconductor is Nb_3Sn (Niobium Tin) and the insulator is C / SiO_2. The poloidal coils employ NbTi (Niobium Titanium) as the superconducting material. The

coolant is supercritical Helium at a temperature of 4.5-5.0 K and a pressure of 0.6 MPa. These two superconductors can withstand magnetic fields in excess of 20T. In addition, both of these superconducting materials are available commercially. Tensile stresses were calculated [14] to be within the ASME limits for each of the magnet systems. The major superconducting magnet parameters of FTWR-SC are displayed in table 5.

Table 5: Superconducting Magnet Parameters

	TF coil	**CS coil**
Conductor	Nb_3Sn	Nb_3Sn
Coolant	Supercritical Helium	Supercritical Helium
Structure	Stainless Steel 316	Incoloy 908
Insulators	C / SiO_2	C / SiO_2
Cross-Sectional Area	0.83 m^2	2.45 m^2
Coolant Temperature	5 K	4.7 K
Field @ Conductor	11.8 T	13.5 T
ASME Allowable S_m	193.33 MPa	193.33 MPa
Tensile Stress	110 MPa	149 MPa
Bore Radius	3.8 m	1.1 m

A wedged design with 18 TF coils was adopted. One unique characteristic of the FTWR / FTWR-SC design is that the TF coils are larger than would be expected for a tokamak of this size, since there must be enough space between the plasma and outer TF coil leg to accommodate the transmutation reactor (see Fig. 1).

To ensure that our TF coil design meets ASME structural design criteria, the various stresses and forces (centering and tensile forces, bending stresses etc.) were evaluated using standard analytic expressions (Appendix C). Table 6 displays the different stresses and forces associated with each magnet system in the FTWR-SC and FTWR. ITER stresses and forces are calculated using the same methods as in the calculations of FTWR-SC and FTWR. The principal reason for the difference in these

values for FTWR-SC and ITER is that ITER has a larger major plasma radius (6.2 m) and a larger toroidal bore (7-8 m).

Table 6: FTWR-SC / FTWR / ITER Stresses & Forces

	FTWR-SC	FTWR	ITER
Centering Force (N)	1.08×10^8	1.75×10^8	5×10^7
Tensile Force (N)	7.29×10^7	4.92×10^7	5×10^7
Bending Stress (MPa)	2.9×10^2	1.81×10^3	5.4×10^2
Solenoidal Coil Tensile Stress (MPa)	149	273	176
Toroidal Coil Tensile Stress (MPa)	110	285	31

** Note: The ASME limits for FTWR [21] (i.e. OFHC magnets) are different then the limits for superconducting magnets

A major portion (28%) of the total ITER R&D is devoted to the magnet systems. ITER has undertaken two R&D projects in order to develop the superconducting magnet technology with high confidence. Therefore, model coils of the TF and CS magnet systems have been developed. The intention of the model coils is to induce the development of the full-scale superconducting technology. The CS model coil has achieved a maximum field of 13 T [20]. The model TF coil was tested at a field of 9.7 T which is slightly lower then the ITER field of 11.8 T.

The central solenoid (CS) coil was designed to produce about 177 Volt-seconds, which, does not take into account any contribution from the PF coil system, hence a conservative estimate. However, this is sufficient to start up the plasma and provide enough volt-seconds for about 13 minutes of burn (flattop) time. If we did include a contribution from the PF coils in the volt-second calculation, an additional 92 V-s (for an additional combined total of 269 V-s) could be achieved which would in turn increase the burn-time from 13 to 25 minutes. This was determined by using equation C.1 (Appendix C), and substituting the flux swing of 25.5 T by 13.5 T, a conservative PF contribution. This computed result, 92 V-s, was then added to the 177 V-s that the central solenoid already had produced. The major design and operational parameters of the TF and CS coil systems are displayed in table 7.

Table 7: Major TF and CS magnetic coil parameters

Parameter	**TF Coils**	**CS Coil**
Conductor	Nb_3Sn	Nb_3Sn
Coolant	Supercritical He	Supercritical He
Field @ Conductor (T)	11.8	13.5
Cross section area (m^2) **coolant fraction (%)** **steel fraction (%)**	0.83 5 36	2.45 5 30
Maximum tensile stress (MPa)	110	149
ASME allowable Sm (MPa)	193	193
Ohmic Heating (MW)	29.7 (all magnets)	21.4
Magnet resistance (Ω)	1.67×10^{-7} (per magnet)	9.37×10^{-9}

III.D Shielding

The other major dimensional change introduced by the use of superconducting magnets is the increased shielding required to protect the magnets from neutron damage. The magnets must be shielded to protect against radiation damage effects of the fusion and fission neutrons, and the heating from secondary gammas. The purpose of the reflector is to redirect escaping neutrons back into the transmutation reactor. The shield-reflector is located just in front of the toroidal field magnets between the magnets and the sources of neutrons from the plasma and the transmutation reactor, and on the top and bottom of the plasma and the transmutation reactor (see Figures 3 and 5). The compositions of the reflector and shield are shown in table 9.

The magnets are designed as lifetime components. Radiation damage limits to magnet insulators of 10^9 rads for organic insulators was used as the design criteria. TWODANT [22] transport calculations determined that the maximum radiation doses in the TF magnets would be 1.37×10^8 rads, which implies that the present shield design would allow the organic insulator dose to be satisfied over the 40 year reactor lifetime. The minimum thickness of the inboard reflector plus shield plus vacuum vessel plus first-wall is approximately 65 cm. Varying the composition of the reflector/shield ratio showed that this is a conservative thickness and the shield could actually be decreased by as much as 11 cm. The same thicknesses are used above and below the plasma and the transmutation reactor and outboard the reactor.

The total thickness inboard of the plasma is 75 cm. This includes 65 cm for the reflector, shield, first wall, and vacuum vessel, plus a 10 cm gap to accommodate the assembly of the components and the plasma scrape-off layer.

The shield thickness has a major impact on the plasma and performance parameters. Several different shield compositions were investigated, and many of them satisfied the overall dose requirements at similar thicknesses (50-85 cm). The FTWR shield composition incorporated into the FTWR-SC design required that the shield be 82.5 cm in thickness. The shield, which was selected, is composed of $W/ZrD_2/B_4C/Pb$ with 10% coolant ($Li_{17}Pb_{83}$) and 10% steel in all regions except for Pb. The shield was chosen because MCNP [23] neutronics analyses that were carried out determined that this combination of the materials was ideal as far as slowing down fast neutrons to medium energies and then to slow energies before capture, in each of the regions, respectively. Additionally, these materials have been investigated in similar applications [24]. The dose requirement can be satisfied with a shield thickness as small as 54 cm for the reference composition. However, a thickness of 65 cm was selected because this dose is a beginning of cycle calculation, with additional fusion neutrons increasing the dose toward the end of cycle. We feel that this is a conservative radial thickness. Additionally, we allowed an extra 10 cm for gaps or additional shielding on the inboard. Since the plasma is shifted outward, we did not otherwise allow for a gap between the circular plasma in our model and the wall on the inboard side. Figure 2 displays the various shield compositions and their dose rates at various thicknesses.

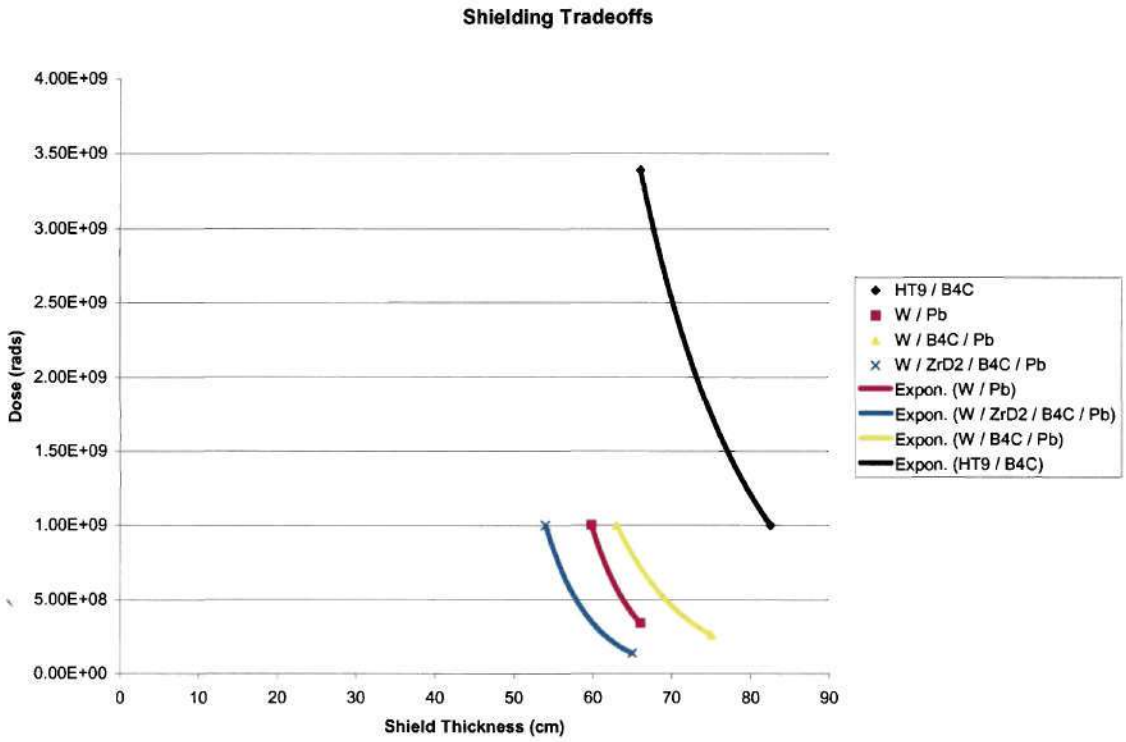

Figure 2: Shielding tradeoff plot which displays the dose to the magnet insulators versus shield thickness for various shield compositions.

A summary of the results elicited from the plot of figure 2 are summarized in table 8.

Table 8: Summary of Shielding Study / Tradeoffs

Shield composition	**Coolant**	**Coolant / Steel Fraction**	**Minimum length to satisfy 10^9 rad dose requirement (cm)**
HT9 / B_4C (FTWR design)	$Li_{17}Pb_{83}$	10% / 10%	82.5
W / Pb	$Li_{17}Pb_{83}$	10% / 10% (in all regions except Pb)	59.8
W / ZrD_2 / B_4C/ Pb (Selected as reference composition)	$Li_{17}Pb_{83}$	10% / 10% (in all regions except Pb)	*54*
W / B_4C / Pb	$Li_{17}Pb_{83}$	10% / 10% (in all regions except Pb)	63

Finally, the details of the reference design shield are given in table 9.

Table 9: Reference Shield Design

Material	Length (cm)	Percent Coolant ($Li_{17}Pb_{83}$)(%)	Percent Structure (HT-9)(%)
W (Tungsten)	15.5	10	10
ZrH (Zirconium Hydride)	15.5	10	10
B_4C (Boron Carbide)**	15.5	10	10
Pb (Lead)	15.5	0	0
Vacuum Vessel	3.0	0	100

*** Boron enriched to 20%*

III.E Radial Build

The radial build of FTWR-SC is significantly different than that of FTWR. The initial change to the radial build was an increase in the thickness of the TF and OH coils. The much larger thickness is associated with the implementation of superconducting magnets. The radial thicknesses of these magnet coils are adopted from the ITER-FEAT design [20].

Additionally, the next consequence of the implementation of superconducting magnets is the radiation damage to the magnet insulators. A thorough shielding investigation was undertaken (III.D), and a shield thickness of 65 cm was found to provide adequate shielding. The minor plasma radius was held at the same value (0.9 m) of the FTWR device. This allows the performance parameters to only be scaled by the percent increase of the major plasma radius. The transmutation reactor remains the same as for the FTWR, in accordance with our initial design objectives. A gap of 10 cm is also maintained between the outer shield and outer TF coil. The radial build of the FTWR-SC is shown in figure 3.

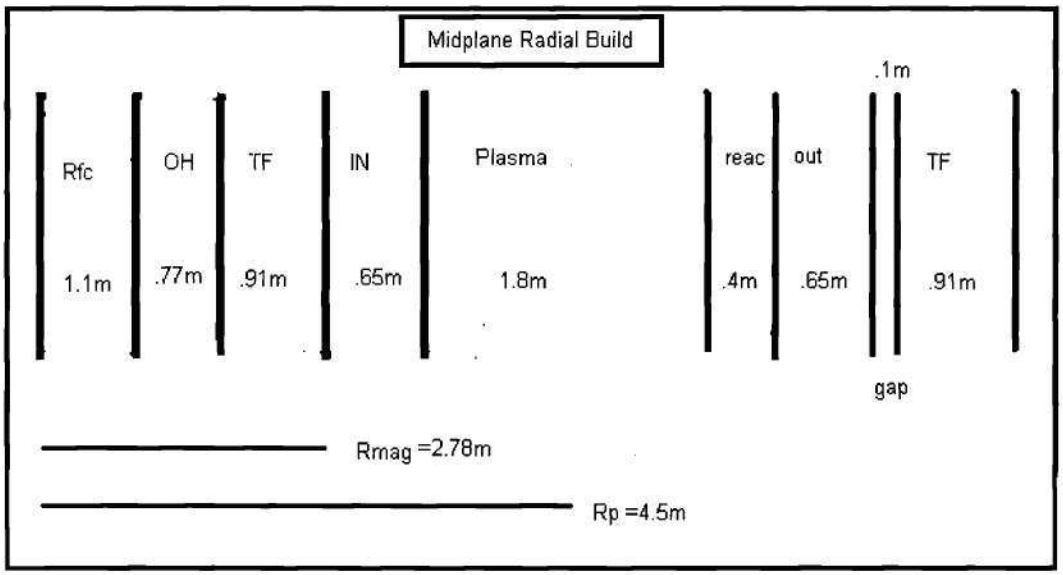

Figure 3: Radial Build of FTWR-SC

R_{fc}= flux core, OH=OH coil, TF=Toroidal Field coil, IN=Inner shield, Reac=Reactor, Out=Outer shield

III.F Plasma Parameters

The superconducting magnets required an increase from FTWR in magnet size, shield size, and the consequence of these increases is an increase in the size of the major plasma radius (III.C, III.D, and III.E). As the radial build of the device is altered, so too are the operating plasma parameters. We choose to operate at the same plasma power density as FTWR, and maintain the same minor plasma radius as in FTWR. As a result,

many of the parameters can be scaled accordingly based upon the percentage increase of the major plasma radius, which is equal to 50%. Therefore, the fusion power increases to 225 MW from the 150 MW value of FTWR. The objective here is to maintain as many of the same plasma values of FTWR, while making appropriate changes to accommodate the superconducting magnets.

The first step in this process was to incorporate the ITER-FEAT magnetic field values into the calculations. A plasma power balance was carried out with all of the same values of FTWR with the exception of the following: P_{fus}(fusion power), κ(plasma elongation), I_p(plasma current), q_{95}(safety factor @ 95% of flux surface), $\langle n \rangle / \langle n_{gw} \rangle$(Greenwald density fraction) and δ(triangularity). The plasma current, fusion power, triangularity, Greenwald density fraction, and elongation are all inputs into the code [25]. The safety factor and many other parameters are calculated as output. Consequently, we observe that initially the leverage we have is within the plasma current, Greenwald density fraction, elongation, and triangularity. This is a result of maintaining a conservative estimate of the bootstrap fraction, which is significantly different for both the FTWR-SC (0.24) and for the FTWR (0.38), and fixing the plasma power density, which is calculated based upon the neutron density and plasma temperature.

The standard design methodology used in the ITER design studies, where the major parameters of the machine (R_0, a, I_p, B_0, etc.) are determined by a relatively small number of equations and assumptions [24,26], was employed. The starting point of this approach is a simple equation for the radial build of the reactor,

$$R_0 = R_{mag} + \Delta_{in} + a \tag{1}$$

where R_{mag} is the major radius at the inner leg of the toroidal field (TF) coil, Δ_{in} is the thickness of the inner shield and reflector region between the plasma and the TF coil and a is the minor radius (see Fig. 3). Using equation (1) along with expressions for the edge safety factor q_{95}, the beta limit and the Greenwald density limit, taking into account the $1/R$ dependence of the toroidal magnetic field, and assuming that the plasma energy confinement time, τ_E, is described by one of the usual confinement scalings such as the ITER IPB98(y,2) scaling [27], an equation can be derived coupling the performance characteristics of the reactor to its major geometric and operational parameters:

$$\frac{(nT\tau_E)_\infty}{1+\frac{5}{Q_p}} = F\left(\beta_N, G_n, \kappa, \delta, q_{95}, \Delta_{RS}, H, A, I_p, B_{TF}, \ldots\right) \tag{2}$$

where $(nT\tau_E)_\infty$ is the value of the triple product $nT\tau_E$ required for ignition (usually taken to be equal to 5×10^{21} m^{-3} keV s for D-T reactors), $Q_p = P_{fus} / P_{aux}$, and F is a nonlinear function of various operating and constraint parameters (see Appendix B). If we select reasonable values for the shape parameters and constraint limits δ, κ, q_{95}, β_N and G_n, and aspect ratio A, we can use equation 2 to perform trade-off studies between the size and the major operational parameters (plasma current and maximum toroidal field), for given performance requirements (Q_p and H).

It should be emphasized here that while most of the physics constraints are inequalities ($\beta_t \leq \beta_{max}$, etc.) they are treated as equalities in our analysis. This means that the performance and power output of the reactor designs obtained via this procedure are the maximum attainable under the assumed constraints. Once the major reactor size parameters (a, R_0, etc.) are fixed, a wide operating space with more modest performance

(Q_p) and fusion powers can be identified by selecting appropriate operating densities and temperatures, or even reducing the plasma current and the toroidal magnetic field.

Based on the results of various scoping studies conducted, a major radius of 4.5 m, corresponding to a maximum field of 11.8 T at the TF coil and a plasma current of 7.2 MA, was selected for our design point. The consequence of this initial investigation is that we cannot operate the FTWR-SC at the same plasma Q and fusion power as FTWR. This initial tradeoff between plasma Q and fusion power led us to increase the fusion power 50% to 225 MW and the following Plasma Operating Contour Plot (POPCON) (figure 4) shows that at this fusion power the plasma Q decreases to 2.0, which was the same as FTWR. In addition, more detailed considerations of the performance characteristics vis-à-vis the neutron source requirements led us to a reference design point with the same size (R_0 = 4.5 m, A = 5.0) but with a slight decrease in the plasma current to 6 MA. This choice represents a reasonable trade-off between low cost (small size and low current).

Taking into account the neutron source requirements of the subcritical fission reactor as well as the relevant increase of the radial build (III.C), a R_0 = 4.5 m design with 6.25 MA current and 11.8 T central magnetic field was selected as the FTWR-SC reference design point. The major radius is a direct consequence of increasing the radial thickness of the TF and CS coils as well as the increase in shield thickness. The central magnetic field of 11.8 T was adopted from the ITER-FEAT design. There are different modes of operation for the ITER device which cause some of the plasma parameters to differ. While some of our trade-off studies had assumed a larger current (>7 MA), the decrease in current optimized the performance parameters of the plasma. The major

plasma-related parameters of the reference design point are listed in table 10. It should be noted that the neutron wall loads for FTWR and FTWR-SC are equal. This is due to the fact that the number of fusions per second has increased by 50% (150 MW to 225 MW), and at the same time the wall area has increased by 50% as well. The profiles used in the following table are the most recent ITER profile assumptions, which are very conservative with respect to the density profile peaking.

Table 10: Reference Plasma Parameters of the Fusion Neutron Source

Parameter	FTWR	FTWR-SC
Major Radius, R_0 (m)	*3.1*	*4.5*
Minor Radius, a (m)	0.9	0.9
Aspect Ratio, A	*3.5*	*5.0*
Plasma Elongation, κ	*1.70*	*1.77*
Plasma Triangularity, δ	0.40	0.40
Safety Factor at 95% flux, q_{95}	*3.00*	*3.09*
Toroidal Field @ R_0, B_0 (T)	*6.1*	*11.8*
Plasma Current, I_p (MA)	*7*	*6*
Normalized Beta, β_N (%)	2.5	2.5
Confinement multiplier, H, ITER IPB98(y,2)	1.1	1.0
P_{fus} (MW)	*150*	*225*
$Q_p = P_{fus} / P_{aux}$	2	2
$\langle n_e \rangle (m^{-3})$	2.0×10^{20}	1.9×10^{20}

Table 10 Continued

$<n_e>/n_{GW}$ (Greenwald density ratio)	*0.75*	*0.80*
$<T_n>$ (keV)	7.60	8.25
Density profile exponent, α_n	0.1	0.05
Temperature profile exponent, α_T	1.0	1.0
Neutron Wall Load (MW/m^2)	0.79	0.79
First Wall Power Density (MW/m^2)	*0.34*	*0.29*
Total DT Fusion Neutron Rate (#/s)	*$5.3x10^{19}$*	*8×10^{19}*
H-Mode Power Flux Margin, P_{sep}/P_{LH}^{thr}	*4.50*	*4.17*
Bootstrap Current Fraction	*0.38*	*0.24*

A POPCON was constructed for the reference design to help us select an appropriate operating point and to scope out the operating range of the machine. It can be seen from Fig. 4 that an operating point with $Q_p = 2$ and $P_{fus} \approx 225$ MW, which satisfies the neutron source performance requirements, is within the allowable operating range. The reference operating parameters at the maximum fusion power of 225 MW and H(y,2) = 1.0 are I = 6 MA, $\beta_N = 2.5\%$, <T> = 8.25 keV, $q_{95} = 3.09$, $n/n_{GW} = 0.8$ and $Q_p = 2.0$, all

of which except Q_p are within the existing tokamak database. The helicity safety factor at 95% of the flux surface is denoted as q_{95}. T indicates the plasma / ion temperature.

The H-Factor (H(y,2)=1.0) is the required energy confinement time enhancement factor, and is computed from the ITER IPB98(y,2) scaling (see Appendix B). We chose a lower H-Factor for FTWR-SC because of our higher Greenwald Density fraction. Experiments have shown that confinement is degraded as we approach this limit, so adopting an H-Factor equal to 1.0 for the FTWR-SC is a reasonably conservative estimate [25].

The following Plasma Operating Contour Plot (POPCON), in figure 5 displays the various plasma parameters of the reference design as a function of plasma density and temperature. It is constructed from the solutions of the steady-state plasma particle and energy balance equations on a density and temperature grid. The POPCON shows contours of constant values of several important plasma power balance parameters, such as the required auxiliary power, the plasma Q: P_{fus}/P_{aux}, the normalized beta:β_n, etc..

The black bullet on the POPCON is the operating point of the FTWR-SC at the maximum fusion power of 225 MW. At this point, it can be observed that the auxiliary power (black curve) is equal to 112.5 MW, which is equal to one-half of the fusion power (magenta curve). Additionally, the normalized beta value of 2.5%, denoted in red, is the normalized ratio of the magnetic field to the plasma pressure. The plasma Q, which is equal to 2 (blue curve), at this point which is simply the ratio of the fusion power to the auxiliary power. The plasma density is equal to 80% of the Greenwald density. The POPCON provides us with the ability to display graphically an operating window for FTWR-SC. Our operating window will be formed below the magenta line (P_{fus}). There

is a great deal of operating margin below the fusion power line, and within the range of values already in the current plasma physics database.

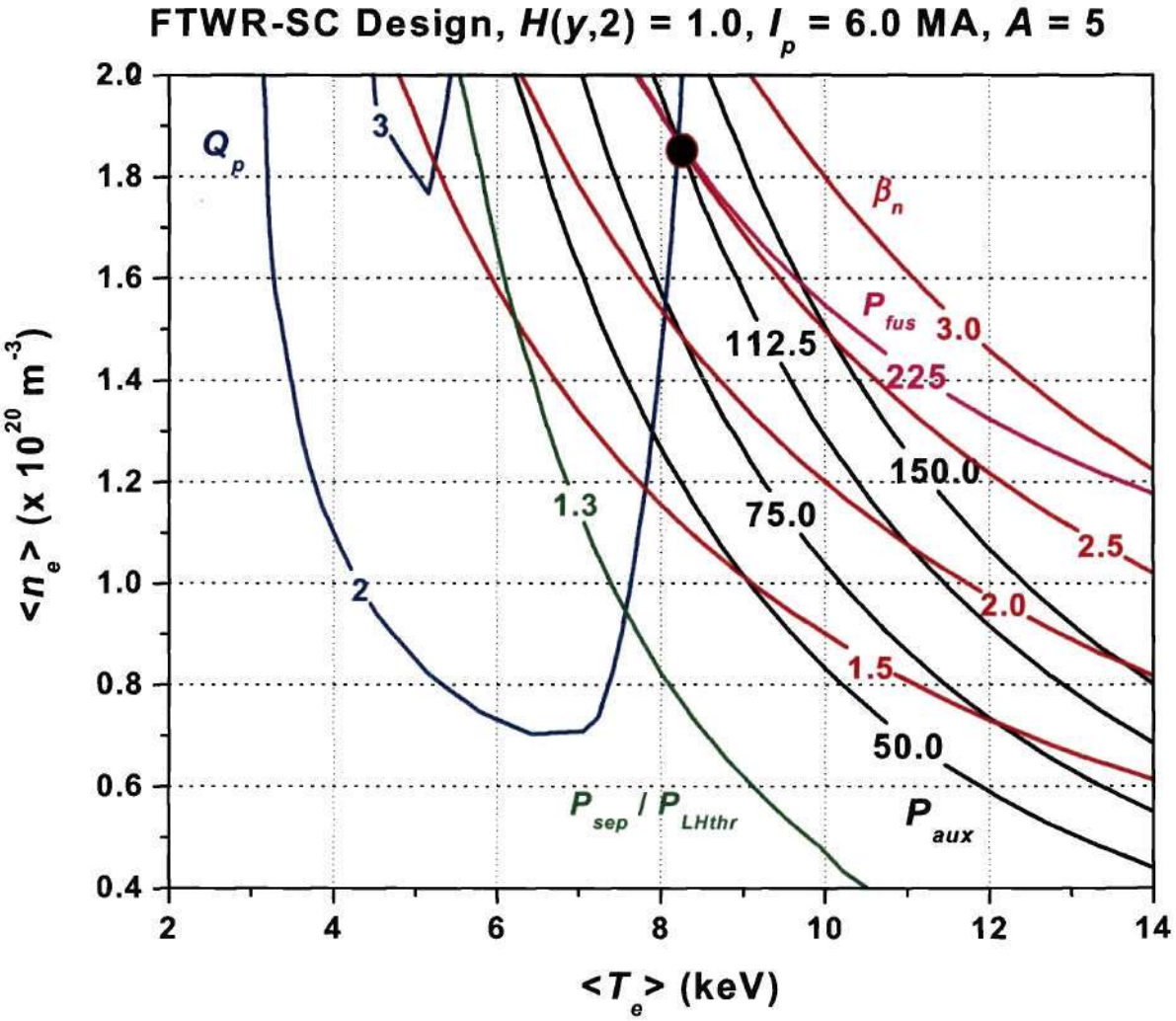

Figure 4: Plasma Operating Contour Plot (POPCON)

The 6 MA / 11.8 T design is also capable of higher performance, if higher levels of confinement or beta limits can be attained. Since the objective of this design is a relatively near-term neutron source to transmute spent nuclear fuel, one of our design

requirements was to remain as close as possible to the present tokamak experimental database. However, even small extrapolations from this database can greatly enhance the performance and hence attractiveness of a fusion neutron source. Such extrapolations allow operation at a higher beta and enhanced confinement level (simultaneous attainment of higher beta and enhanced confinement is usually required) and result in higher fusion power densities and higher bootstrap current fractions. Tokamaks operating under these improved conditions are usually called *Advanced Tokamaks*, and are being vigorously studied by the fusion community [29]. Several tokamak experiments around the world have achieved advanced tokamak operation for short pulses, and this database is rapidly growing.

III.G Current Drive

Steady-state operation is one of the goals of the FTWR-SC design. This means that external current drive will be required to supply part of the plasma current in the fusion reactor core. Since most current drive methods for reactor-grade plasmas are rather inefficient and expensive, every effort should be made to minimize the external current drive requirements by maximizing the bootstrap current fraction. For the reference design point, this fraction is estimated to be about 24 % using a simple scaling formula (Appendix B). However, it is believed that higher bootstrap currents can be attained by optimizing various plasma profiles.

To get an idea of the influence of the bootstrap current fraction on the demands on the current drive system, the current drive efficiency $\eta_{CD} \equiv I_{CD}/P_{CD}$ (Amps/Watt) required for steady state operation is calculated for our reference design for two values of the

plasma Q_p. This calculation assumes that all of the auxiliary power injected into the plasma is also available to drive current, therefore $I_p\left(1-f_{bs}\right)=\eta_{CD}\,P_{fus}/Q_p$. The reference values for fusion power and plasma current (225 MW and 6 MA respectively) have been assumed.

Table 11: Current Drive Efficiencies required for steady-state operation for various bootstrap fractions.

Bootstrap Current Fraction	η_{CD} (A/W), $Q_p = 2$
0.2	0.043
0.4	0.032
0.6	0.021
0.8	0.011

It can be seen from table 11 that for the reference design point, a current-drive efficiency in the range of 0.03 – 0.04 A/W would be necessary to achieve steady-state operation. Although a detailed analysis of the current drive and heating system of this design has not been performed, a system based on fast waves (FW) in the ICRF regime for central current drive and lower hybrid (LH) waves for off-axis drive would be a reasonable choice [30].

An estimate of the FW current drive efficiency of such a system can be obtained by using a simple scaling formula developed for the ARIES RS design study [30,31]. For our reference design point, this simple scaling predicts a current drive efficiency of 0.04 A/W, resulting in a driven current of 5.6 MA, 0.4 MA less than the 6 MA that are needed.

We can drive the full 6 MA by optimizing the plasma profiles to increase the bootstrap current fraction and/or by operating at a slightly lower Q and higher temperature to increase current drive power and efficiency. A fraction of the current would be driven by LH, which has a higher current drive efficiency than ICRF FW.

Furthermore, even if all the current had to be driven by FW current drive, we could operate at higher temperatures and lower densities to increase the current drive efficiency. As can be seen from the POPCON plot in Fig. 5, by moving along the 225 MW fusion power line, we can produce the same amount of fusion power at higher temperatures and lower densities. We would have to accept slightly lower Q_p operation, but this also works to our advantage in this case since the extra auxiliary power would be available to drive more current.

It should also be mentioned that intensive research is being carried out in the area of tokamak current drive, and the relevant experimental database is rapidly growing [32]. More efficient methods, such as Electron Cyclotron (EC) current drive, may soon be available.

III.H Power & Performance Analysis

In contrast to FTWR, which operated at electric power break-even because power was dissipated in ohmic heating, the FTWR-SC operates with an electric power surplus. The extent of excess power of the design is characterized by the electric power amplification factor, also known as the engineering "Q" of the reactor, which is just the inverse of the recirculating power fraction, being at least unity:

$$Q_e = \frac{\text{Gross Electric Power Produced}}{\text{Gross Electric Power Consumed}} \geq 1 \tag{4}$$

The gross electric power produced, P_{EG}, is given by

$$P_{EG} = \eta_{th}\left[P_{fus}\left(\frac{1}{5}+\frac{1}{Q_p}\right)+P_{reac}\right] \tag{5}$$

where the first term represents the power deposited on the plasma facing components (mainly charged particles and radiation) and P_{reac} represents the total power (including the fusion neutron contribution) deposited in the transmutation reactor region (predominantly fission power).

The total electric power consumed by the power plant in order to operate its various components, P_{plant}, is then given by

$$P_{plant} = \frac{P_{fus}}{\eta_{CD}^{e} Q_p} + P_{tot}^{TF} + P_{tot}^{CS} + P_{tot}^{PF} + P_{p-FW} + P_{p-reac} + P_{repro} + P_{BOP} + P_{other} \tag{6}$$

where η_{CD}^{e} is the wall-to-plasma electric efficiency of the current drive and heating system. P_{repro} is the power required to reprocess fuel on site, P_{BOP} is the balance-of-plant power, $P_{p\text{-}reac}$ is the total pumping power for the transmutation reactor, $P_{p\text{-}FW}$ is the pumping power for the first wall and P_{other} accounts for miscellaneous powers that are not accounted for explicitly.

Values for these powers and efficiency factors for the FTWR-SC reference design are shown in table 12. Most of these values are calculated. However, some numbers (η_{th}, P_{repro}, P_{BOP}, P_{other}) have been estimated by direct scaling from comparable design studies. P_{repro} and P_{BOP} were estimated from a cost estimate of these same facilities for an ATW design [33]. It should be noted that the refrigeration power for FTWR-SC is essentially negligible.

Table 12: Reference Design Powers & Efficiencies

P_{fus} (MW)	225
P_{reac} (MW)	4275
$P_{refrig}(MW)$	17×10^{-3}
$P_{htg\text{-}CD}$(MW)	112
$P_{p\text{-}FW}$ (MW)	4
$P_{p\text{-}reac}$ (MW)	197
P_{repro} (MW)	34.5
P_{BOP} (MW)	9
P_{other} (MW)	10
η_{th} (%)	40
η^{e}_{CD} (%)	70

Using these values, the calculated electric power amplification factor Q_e for the reference design is about 5.0, i.e. the FTWR-SC produces all the electricity that it needs to perform its mission, transmuting spent nuclear fuel, along with an electricity surplus.

CHAPTER IV. FTWR-SC DESIGN SUMMARY

IV.A Geometric Configuration and Materials

The geometric configuration of the FTWR-SC is shown in figures 3 and 5. The transmutation reactor consists of a ≈ 40 cm thick ring of vertical hexagonal fuel

assemblies located outboard of the plasma chamber of the tokamak fusion neutron source. The reactor metallic fuel consists of a zirconium alloy containing transuranics from SNF dispersed in a zirconium matrix and clad with a steel similar to HT-9. The coolant for the reactor, reflector and shield, first-wall and divertor is Li17-Pb83 eutectic enriched to 20 % ^{6}Li to meet the tritium self-sufficiency requirement. Reflector and shield are located inboard of, above and below the plasma chamber and above, below and outboard of the reactor to protect the magnets from radiation damage and to reflect neutrons towards the reactor. The toroidal and solenoidal magnets employ Niobium-Tin (Nb_3Sn) as the superconductor while the poloidal magnets employ Niobium-Titanium (NbTi), and each magnet system utilizes supercritical Helium as the coolant. The materials composition of the FTWR-SC are the same as for the FTWR except as otherwise indicated by italics and are summarized in table 13.

Table 13: Materials Composition of FTWR-SC

Component	Material
Reactor	
Fuel	Zr-transuranic alloy in Zr matrix
Clad & Structure	HT-9-like steel
Coolant	Li17Pb83 (^{6}Li enrich 20%)
Reflector	HT-9, Li17Pb83
Shield	*W / ZrD_2 / B_4C / Pb*
Magnets	
Conductor	*Nb_3Sn, NbTi*
Coolant	*Supercritical Helium*
Structure	*Stainless Steel 316, Incoloy 908*
Structure	HT-9-like steel
Coolant	Li17Pb83

IV.B Major Design Parameters

The neutron source is a D-T tokamak with the parameters shown in table 14, most of which are in the range routinely achieved on operating tokamaks [26]. The only two parameters which are not within this range are the plasma energy amplification factor Q_p and the steady-state pulse length. The required value of Q_p is only a factor of about 2 greater than what has been achieved on the Joint European Torus (JET) device, and there is a proposal for $Q_p \approx 2$ operation in JET. Perhaps the greatest advance beyond the present state of the art in tokamak operation is the steady-state pulse length. Using a conservative estimate of a current drive efficiency $\eta_{CD} = 0.04$ A/W, we estimate that steady state current maintenance could be achieved with $Q_p = 2.0$, at 225 MW fusion power. Figure 5 illustrates the geometric configuration of FTWR-SC, which is identical to that of FTWR with the exception of dimensions.

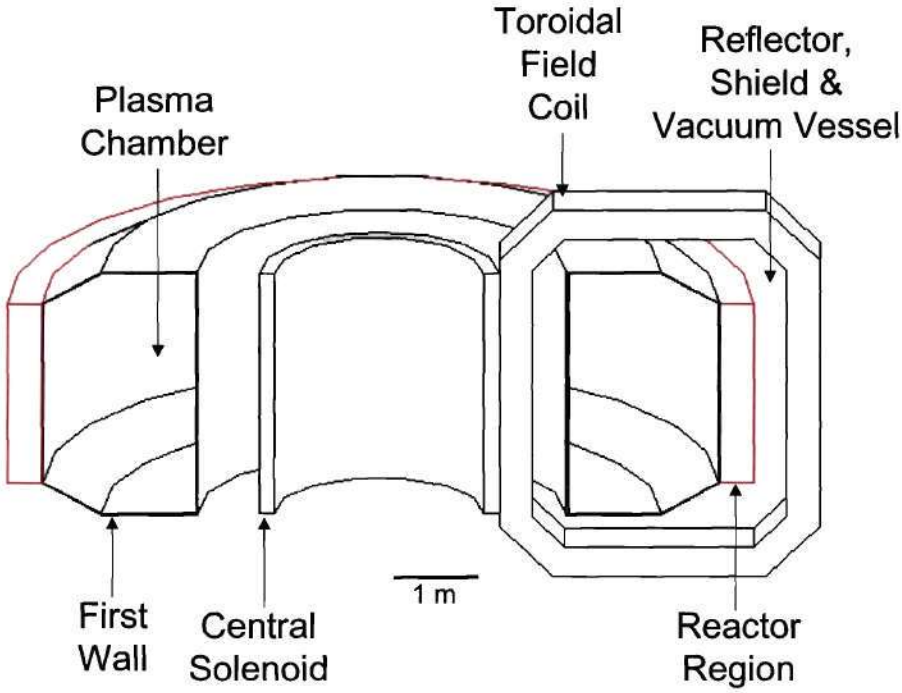

Figure 5: Schematic of Geometric Configuration of FTWR-SC

Allowing 0.9 m for the plasma radius and 0.17 m for inboard scrape-off layer plus vacuum vessel plus gaps, 0.65 m for the reflector-shield and 2.85 m for the magnet system results in an increase of major radius from 3.1 m in FTWR to 4.5 m in FTWR-SC. The aspect ratio of 5.0 is similar to the ARIES-I Tokamak Reactor [31]. The overall radial build of the reactor has changed significantly between the FTWR and FTWR-SC designs. We have increased all of the thicknesses except for the reactor and gap regions which maintain the same thickness. The flux core radius is determined from the following equation: $R_{fc} = (\sqrt{((\Delta\Phi)_{req} / \pi B_{OH})})x\ 1.1$. This equation is multiplied by a factor of 1.1 to ensure that we have 10% more volt-seconds than required. The radial thickness of the CS and TF coils are adopted from the ITER-FEAT design. The inner and outer shield thicknesses were determined as sufficient to satisfy lifetime dose

requirements to the magnet insulators, using the TWODANT neutron transport code as well as monte carlo simulations. As a result of increasing the size of the magnets and the thickness of the shield, an increase in the major radius was also a consequence. The major radius increased from 3.1m in FTWR to 4.5m in the FTWR-SC. The minor radius remains the same at 0.9m.

The increase in the major radius from FTWR to FTWR-SC is equal to 50%. This causes a 50% increase in reactor volume, as well as a 50% increase in plasma volume. The principal plasma parameters of FTWR remain the same, thus FTWR-SC has the same plasma power density. The fusion power is increased by 50% to 225 MW. Likewise, we choose to have the same transuranic density, power density, and volumetric transmutation rate as in FTWR. Additionally, we have a 50% increase in transuranic loading, power, and transmutation rate.

The FTWR-SC magnetic system design is based on the design of the ITER-FEAT system. The magnetic field levels are well within the range of existing tokamaks. The lifetime radiation and neutron doses to the toroidal field coils are intended to be below the limit for organic insulators, although these limits are not well defined. The central solenoid produces a flux swing of 177 Vs, based on a field inversion in the CS from 13.5 T to -12 T but not including any contributions from the poloidal field coils. For the 6 MA reference case, this flux variation is sufficient for plasma start-up and a 13 minute current flat top.

The FTWR-SC first-wall design is an adaptation of the ITER design [16], albeit with HT-9-like steel structure. Although the qualification of HT-9-like steel for operation in a neutron irradiation environment is in progress, the radiation damage limit

is not yet known. However, we believe that this limit will probably allow about 5-10 (623 day) cycles (> 100-200 dpa) before it is necessary to replace the first-wall of the neutron source. The neutron source parameters of FTWR-SC are displayed in table 14.

Table 14: Neutron Source Parameters

Parameter	Value
Plasma	
Major radius, R_0 (m)	*4.5*
Minor radius, a (m)	*0.9*
Elongation, κ	1.77
Magnetic field, B_0 (T)	*7.5*
Plasma current, I_p (MA)	*6*
Bootstrap current fraction	*0.24*
Normalized beta, β_N (%)	2.5
Confinement factor, H ITER IPB98(y,2)	1.0
Fusion power (MWth)	*225*
Plasma energy amplification, Q_p	2.0
Pulse length	steady-state
Magnets	
Toroidal field @ coil (T)	11.8
Central solenoid field @ coil (T)	13.5

Table 14 Continued

Inductive flux (V-s)	177
Temperature (K)	4.7-5.0
Power dissipation & refrigeration (kWe)	*13*
Lifetime radiation dose (rads)	1.37×10^8
First-Wall	
14 MeV neutron wall load (MW/m^2)	*0.79*
Surface heat load (MW/m^2)	*0.29*
Radiation damage (dpa/623 d cycle)	21
Tritium Inventory (liquid breeder / solid breeder)	
Beginning of cycle (kg)	*0.27 / 16.53*
Maximum (kg)	*1.64 / 18.60*

The main parameters of the transmutation reactor are given in table 15. The design is an adaptation of the ANL design of a transmutation reactor for an accelerator (ATW) neutron source [18], which has a fast neutron spectrum to maximize the fission probability per neutron absorbed in transuranics.

Table 15: FTWR-SC Transmutation Reactor Parameters

Parameter	Value
Maximum multiplication constant, k_{eff}	0.95
Actinide loading (MT)	*40.5*
Maximum actinide enrichment (V/O)	45
# Hexagonal fuel assemblies	*705*
Fuel assembly pitch (cm)	16.1
Fuel assembly length (cm)	228
Fuel pin diameter (cm)	0.635
Average power density (kW/liter)	124
Fuel cycle	4 batch
Clad irradiation @ discharge (dpa)	150
Coolant Tin/Tout (K)	548/848
Coolant flow velocity (m/s)	0.76
Coolant mass flow rate (kg/s)	77445
Coolant pumping power (MWe)	196.5

IV.C Performance Summary & Tritium Inventory

The power output and transmutation rate of the FTWR-SC can be scaled from the FTWR values since $P_{th} \sim TR \sim P_{fus}/(1-k)$, where $k = k_\infty (1-L(1-R))$ is the neutron source multiplication factor. The same composition and height and width of the annular core are specified for the FTWR-SC and FTWR, so k_∞ and the leakage (L) are the same for both. For the purposes of this paper we assume that the reflection probability (R) is also the same; hence $P_{th} \sim TR \sim P_{fus}$. Thus, the FTWR-SC and FTWR have the same core power density of 124 kW/liter.

If the FTWR-SC and FTWR plasmas operate at relatively the same temperature and density, the power in FTWR-SC is about 50% greater (4500 MW_{th}) than in FTWR. The fusion power (225 MW) and neutron source (8.0×10^{19} #/s) are also 50% greater. The FTWR-SC would have a 50% greater actinide loading (40.5 MT) and would operate on the same 4-batch fuel cycle as the FTWR [1], destroying the actinide content of spent nuclear fuel at the rate 153 MTU/FPY. The LWR support ratio of the FTWR-SC would be 50% greater than for the FTWR, or 4.5 GW_e-LWR/FTWR-SC.

With $\eta_{th} = 40\%$, the FTWR-SC would produce 1800 MW_e. The power required to operate the FTWR-SC is 365 MW_e, which leaves a net electrical power production of 1435 MW_e (Q_e =5.0). The FTWR design had a $Q_e = 1.0$ which did not yield an electricity surplus. The major performance parameters of FTWR-SC are summarized in table 16.

Table 16: Major Performance Parameters of FTWR-SC

Parameter	Value
Total Power (MWth)	*4500*
Thermal-to-electrical conversion (%)	40
Fusion Neutron Source Strength (#/s)	*8×10^{19}*
SNF Transmutation Rate (MTU/FPY)	229.5
Transuranic Mass Reduction in SNF (%)	99.4
Support Ratio (GWe LWR/FTWR-SC)	*4.5*
Electrical Power Amplification, Q_e	*5.0*
Lifetime (FPY)	40
Availability (%)	60

The transmutation fuel cycle is same for FTWR-SC as for FTWR. Thus, the toxicity (defined as the volume of water required to dilute the SNF to the maximum permissible concentration for human consumption) of the original SNF from a once-through LWR cycle and the toxicity from the same SNF after transmutation in a FTWR-SC (without the uranium, which is assumed to be recovered and disposed of as low level waste in both cases) are the same for both devices. These toxicities are compared with the toxicity of the original as-mined uranium ore from which the fuel was fabricated in Fig. 6. The toxicity of the LWR SNF including the uranium is also shown to illustrate the effect of just removing the uranium from the SNF. The SNF from the LWR becomes less

toxic than the natural as-mined uranium ore from which it was fabricated in about 7,500 years. If this same SNF were irradiated in the FTWR-SC, it would become less toxic in about 500 years than the natural as-mined uranium ore from which it was fabricated. While toxicity is only one of many measures of the hazard potential of radioactive waste, this comparison does indicate the magnitude of the benefit of the transmutation of SNF.

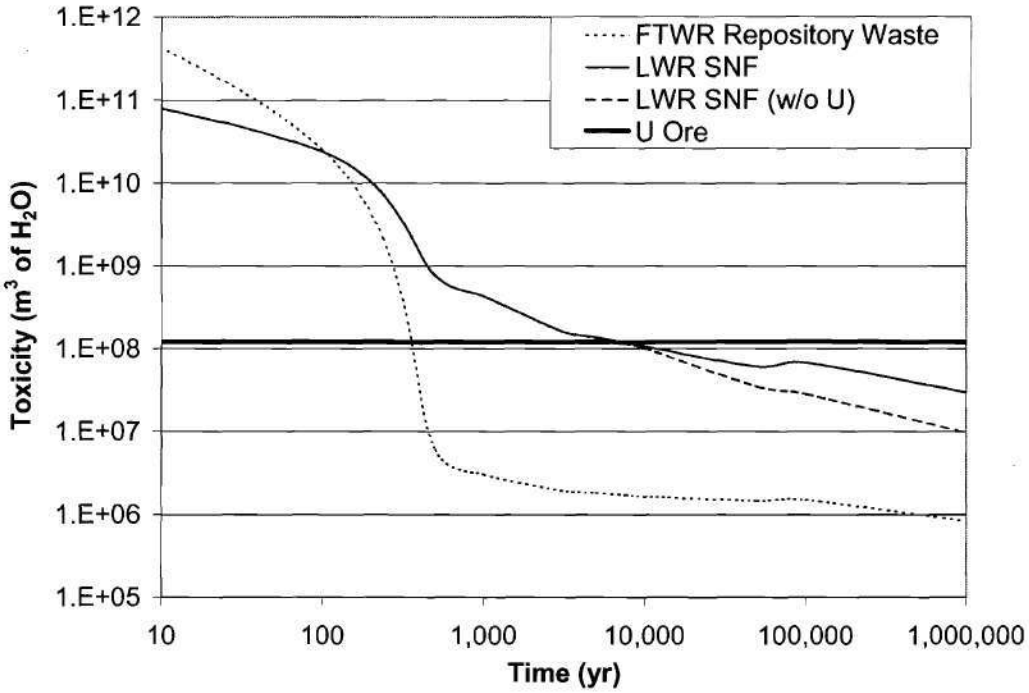

Figure 6: Toxicity of SNF (uranium recovered) with and without transmutation in FTWR-SC compared to toxicity of natural uranium ore.

The beginning of cycle (BOC) inventory is a function of the fusion rate and the operating parameters of the tritium system. We used a simple estimate of the beginning of cycle tritium inventory--a tritium inventory equivalent to the total number of fusions occurring in the first 30 full power days of operation must be available at the beginning

of each cycle. The BOC tritium inventory for the reference fuel cycle of the liquid breeder is 0.27 kg, which is 50% then that of FTWR. Additionally, the maximum tritium inventory is 1.64 kg. As for the solid breeder the BOC inventory is 16.53 kg and peak inventory is 18.60 kg.

IV.D FTWR-SC / FTWR Parameter Comparison

While many of the performance parameters remain close to or the same as the corresponding values in each device, the following comparisons highlight three major differences / improvements between FTWR/FTWR-SC. The FTWR design yielded stresses at the ASME limits which are not generally as conservative as we would desire, while FTWR-SC stresses at the magnet coils are significantly below the ASME limits. Additionally, the large ohmic heating losses of FTWR do not exist in FTWR-SC. As stated in the initial design objectives the FTWR-SC is designed to produce electricity, while FTWR was designed for self-sufficiency in electricity production. Table 17 compares the various overall characteristics of FTWR-SC & FTWR.

Table 17: FTWR-SC / FTWR Parameter Comparison

Symbol	Parameter	FTWR-SC	FTWR
A (R_o/a)	Aspect Ratio	5.00 (4.5/0.9)	3.48 (3.1/0.9)
I_p (MA)	Plasma Current	6.00	7.00
K	Elongation	1.77	1.70
Δ	Triangularity	0.40	0.40
B_o (T)	Magnetic Field @ Plasma Center	7.48	6.10
H-Factor	Confinement Enhancement	1.00	1.10
P_{fus} (MW)	Fusion Power	225	150

Table 17 Continued

P_{nw} (MW/m^2)	Neutron Wall Load	0.79 (225MW / 284.8m^2)	0.79 (150MW /189.9m^2)
P_{thw} (MW/m^2)	Thermal Power to first Wall	0.291	0.270
f_{BS}	Bootstrap Fraction	0.24	0.38
n_{avg} (10^{20}m^{-3})	Average Neutron Density	1.9	2.0
S (#/sec)	Neutron Source Strength	8.00 x 10^{19}	5.32 x 10^{19}
β_n (%)	Normalized Beta	2.5	2.5
n/n_{GW}	Greenwald Density Ratio	0.80	0.75
q_{95}	Safety Factor @ 95% Flux Surface	3.09	3.00
Q_p (P_{fus} / P_{aux})	Plasma Q	2.0	2.0
Q_e	Electric Power Amplification Factor	5.0	1.0

CHAPTER V. CONCLUSIONS & DISCUSSION

The following conclusions of this thesis differentiate FTWR-SC from the FTWR. First of all, the extra thickness of the superconducting magnet, relative to the normal magnet design of FTWR, as well as the extra shielding required to protect the superconductor from radiation damage increases the major plasma radius by 50%, from 3.1 m for FTWR to 4.5 m in FTWR-SC. Additionally, as a result of retaining relatively the same operating plasma temperature and density, and the same nuclear core design and fuel cycle as in FTWR, we have a 50% increase in power, nuclear transmutation rate, transuranic loading, coolant mass flow, tritium inventory, etc.. The increase in the major radius can be traded off by a reduction in the plasma current while maintaining the same plasma confinement and stability margins. This translates into an increased inductive current drive capability. Since the superconducting magnets are based on the ITER design and the technology supported by ITER R&D, and since the plasma parameters (β_n=2.5%, H=1, Q_p=2) are almost identical to those of FTWR, the conclusions reached in the FTWR study also hold for FTWR-SC.

The first of these conclusions adopted from the FTWR study is that a Superconducting Fusion Transmutation of Waste Reactor (FTWR-SC) based on Liquid Metal—Metal Fuel Fast Reactor technology and a D-T tokamak fusion neutron source is a feasible option for substantially reducing the quantity and hazard potential of high-level radioactive waste from spent nuclear fuel (SNF) that must be stored in geological repositories. A FTWR-SC which produces 4500 MWth would transmute the transuranic content of about 150 metric tones of SNF per full-power-year and would be self-sufficient in producing all the tritium and electricity required for its operation. By

repeated recycle of transuranics from SNF in a series of FTWR-SCs, more than 99 % of the transuranics would be destroyed by fission. One FTWR-SC operating with 60% availability would 'support' 4.5 commercial Light Water Reactors (LWRs, 1000 MWe each), so that an equilibrium fleet of 23 FTWR-SCs (4500 MWth each) would support the present US commercial nuclear capacity of 100 GWe. In FTWR the equilibrium fleet size was 34. This same support level applies also to a mix of FTW and ATW reactors.

The second major conclusion is that a fusion neutron source that meets all the requirements, except high availability, for a FTWR-SC could be designed and built today, based on the existing tokamak physics and fusion technology databases. The plasma confinement and stability parameters needed in a FTWR-SC ($H \geq 1$, $\beta_N \approx 2.5$) are routinely achieved in operating tokamaks. The required plasma current, plasma energy amplification factor and auxiliary heating power ($I_p = 6$ MA, $Q_p = 2$, $P_{aux} \approx 112.5$ MW) are only modest extrapolations from existing tokamaks. Empirical scaling laws predict that steady-state current drive can be achieved with these parameters, based on experience in existing tokamaks. The tritium processing system technology that has been developed for JET and TFTR and in the ITER R&D program should provide an adequate design base for the FTWR-SC. The remote handling technology that has been developed in the ITER R&D program should provide an adequate design base for the fusion neutron source for the FTWR-SC.

The third major conclusion is that availability is the major issue for the FTWR-SC. The equilibrium transuranic inventory (hence the repository requirement) and the size of the FTWR-SC fleet needed to achieve this equilibrium inventory are sensitive to the availability of the FTWR-SC. Achieving an availability of > 50% in the second

generation of FTWR-SCs is important. Since we have based the FTWR-SC design on the nuclear and processing technology that is being developed in the US fast reactor program for the ATW, we assume the same high availability for the transmutation reactor in the FTWR-SC as is anticipated in the ATW design. Thus, the availability of the FTWR-SC will be determined by the availability of the fusion neutron source.

There are two elements to the issue of availability of the fusion neutron source: 1) reliable, high availability, routine operation of the neutron source and 2) downtime for the replacement of failed components. Both of these issues suggest the need to build a prototype tokamak fusion neutron source as soon as possible to learn how to achieve routine high availability operation and to learn about any short-term failure modes of the components.

This leaves the issue of long term component failure due to radiation damage, which is common to all transmutation reactors and other devices with a high neutron fluence mission. The most inaccessible components in the FTWR-SC, the toroidal and central solenoid magnets, are shielded sufficiently to be lifetime components. However, some structural components (e.g. the first-wall of the neutron source and the clad and structure in the reactor fuel assemblies) will accumulate high levels of radiation damage. The radiation damage limit for the HT-9-like steel components is not known, but estimated lifetimes in a fusion neutron spectrum are in the range 100-200 dpa. These damage limits would require that first-wall of the fusion neutron source be replaced 2-4 times during the 40 FPY lifetime of a FTWR-SC. Since the wall replacement could be scheduled to coincide with a plan outage for refueling it should not have a substantial impact on average lifetime availability, even if first-wall lifetimes < 100 are encountered.

We tried to make this initial assessment of a FTWR-SC realistic by basing the design concept for the neutron source on the existing tokamak physics and fusion technology databases and by basing the design concept for the transmutation reactor on the nuclear and processing technology that is being developed for the ATW reactor. The major uncertainties in this existing database vis-à-vis the FTWR-SC requirements are in the areas of high availability, steady-state tokamak operation and structural materials lifetime, as discussed above, and only the former would substantially impact availability. However, there will inevitably be design-specific R&D requirements identified by a more detailed assessment of the FTWR-SC at the conceptual design level that includes the mechanical and thermal designs of the magnet systems, the transmutation reactor, the fuel changeout and reprocessing systems, etc. and the safety and environmental analysis.

CHAPTER VI. Appendices

APPENDIX A - MATERIALS PROPERTIES

COOLANTS

Properties	Li17PB83	LBE
	[35]	[36]
Density (kg/m^3)	9270	10190
Resistivity (Ω-m)	9.71×10^{-8}	4.29×10^{-7}
Specific Heat, C_p (J/kg -°K)	187	129
Viscosity (mPa-s) @ 698 °K	1.39×10^{6}	1.46×10^{6}

HT-9 [37]

Property	Value
Yield strength (MPa)	307
Ultimate strength (MPa)	396
Thermal conductivity (W/m-°K)	30
Poisson's ratio	3
Density (kg/m^3)	9270
Resistivity (Ω -m)	1.32×10^{-6}

NbTi [38]

Property	Value
Critical Temperature (K)	10
Critical Magnetic Field (T)	15

Nb_3Sn [38]

Property	Value
Critical Temperature (K)	18
Critical Magnetic Field (T)	24.5

Supercritical Helium [38]

Property @4.7 K	Value
Density (kg/m^3)	113.3
Specific Heat, C_v (kJ/kg -°K)	2.64
Pressure (MPa)	0.153

APPENDIX B – PLASMA PHYSICS ANALYSIS

Confinement [28]

The ITER Database IPB98(y,2) scaling is used:

$$\tau_E = H\tau_E^{IPB98(y,2)} \tag{B.1}$$

where

$$\tau_E^{IPB98(y,2)} = 0.144 I_p^{0.93} B_0^{0.15} P^{-0.69} \overline{n}_{e20}^{0.41} M^{0.19} R_0^{1.97} A^{-0.58} \kappa^{0.78} \tag{B.2}$$

and the units are in s, MA, T, MW, 10^{20} m^{-3}, amu and m.

Greenwald Density Limit

$$\overline{n}_{e20} \leq \frac{I_p\,(\mathrm{MA})}{\pi a^2} \tag{B.3}$$

L-H mode transition threshold [28]

$$P_{LH}\,(\mathrm{MW}) = (2.84/M)\, B_0^{0.82} \overline{n}_{e20}^{0.58} R_0 a^{0.81} \tag{B.4}$$

MHD Stability

$$\beta_t \equiv \frac{\langle n_e T_e + n_i T_i + p_\alpha \rangle}{\dfrac{B_0^2}{2\mu_0}} \leq \beta_N \frac{I_p\,(\mathrm{MA})}{a B_0} \tag{B.5}$$

$$q_{95} = \frac{5a^2 B_0}{R_0 I_p} \frac{1+\kappa^2\left(1+2\delta^2-1.2\delta^3\right)}{2} \frac{\left(1.17-\dfrac{0.65}{A}\right)}{\left(1-\dfrac{1}{A^2}\right)^2} \geq 3 \tag{B.6}$$

Bootstrap Current Fraction [39]

$$f_{bs} = C_{BS}\left(\sqrt{\varepsilon}\beta_p\right)^{1.3} \tag{B.7}$$

where

$$C_{BS} = 1.32 - 0.235q_{95} + 0.0185q_{95}^2 \tag{B.8}$$

and

$$\beta_p = \beta_t\left(B_0/B_p\right)^2, \quad B_p = \frac{I_p\left(\mathrm{MA}\right)}{5a\sqrt{\frac{1+\kappa^2}{2}}} \tag{B.9}$$

Fast Wave ICRF Current Drive Efficiency [30]

$$\gamma_{FW} \equiv R_0 n_{e20}\eta_{CD} = 0.062T_e\left(\mathrm{keV}\right)^{0.56} \tag{B.10}$$

where $\eta_{CD} = I_{CD}$ (MA) / P_{aux} (MW) is the current drive efficiency.

Volt-Second Analysis

Volt-seconds required for startup, $\Delta\Phi_{start} = (\Delta\Phi)_{ind} + (\Delta\Phi)_{res}$ where:

$$\left(\Delta\Phi\right)_{ind} = I_p L_p \tag{B.11}$$

$$\left(\Delta\Phi\right)_{res} = C_{Ejima}\mu_0 R_0 I_p \tag{B.12}$$

where the Ejima coefficient is assumed to be equal to 0.4 [39].

$$L_p = \mu_0 R_0\left[\ln\left(\frac{8R_0}{a\sqrt{\kappa}}\right) + \frac{l_i}{2} - 2\right] \tag{B.13}$$

and the internal inductance l_i is given by [40]:

$$l_i = \ln\left(1.65 + 0.89\left(q_{95} - 1\right)\right) \tag{B.14}$$

APPENDIX C - MAGNET ANALYSIS

Central Solenoid (CS) Coil

Volt-seconds:

$$(\Delta\Phi)_{cs} = \pi \Delta B_{OH} R_{fc}^2 \left[1 + \Delta_{OH} / R_{fc} + 1/3 \, (\Delta_{OH} / R_{fc})^2 \right] \quad \text{(C.1)}$$

B_{OH} : magnetic field at the central solenoid (flux swing from -13.5 T to 12 T which is equal to 25.5 T)

R_{fc} : flux core radius

Δ_{OH} : radial thickness of central solenoid

Equation C.1 assumes linear decay of the magnetic field within the CS cross section.

Tensile Stress [41]:

$$\sigma_{CS} = \frac{B_{OH}^2}{2\mu_0}\left(\frac{R_{fc}}{\Delta_{OH}} + \frac{1}{3}\right) \leq S_m \quad \text{(C.2)}$$

where according to the ASME code, S_m = min [1/3 ultimate stress, 2/3 yield stress]. For composite materials, the maximum stress S_m is estimated from:

$$S_m = \sum_i f_i \times S_{mi} \quad \text{(C.3)}$$

where S_{mi} is the maximum allowable stress of material i and f_i is the volume fraction of material i.

Toroidal Field (TF) Coils

Centering Force [41, 42]

$$F_R = \frac{\mu_0 N I_{TF}^2}{2}\left[1 - \frac{1}{\sqrt{\left(1-\varepsilon_p^2\right)}}\right] \tag{C.4}$$

N : number of TF coils

I_{TF} : current per TF coil

and $\varepsilon_p = R_{bore} / R_0$ where R_{bore} the radius of the magnet bore.

Bending Stress

$\sigma_{bend} = F_R / A_{in}$ where A_{in} is the area of the inner leg of the magnet over which the inward force acts.

Tensile Force [41,42]

$$F_T = \frac{1}{2}\frac{\mu_0 N I_{TF}^2}{4\pi}\ln\left(\frac{1+\varepsilon_p}{1-\varepsilon_p}\right) \tag{C.5}$$

and the corresponding tensile (hoop) stress is equal to

$$\sigma_t = F_T / A_{tor} \tag{C.6}$$

where A_{tor} is the cross sectional area of conductor plus structure, but not including the coolant channels.

According to the ASME code, $\sigma_t + \sigma_{bend} \leq 1.5S_m$ where S_m is defined as above.

APPENDIX D - DEFINITION OF TERMS

ANL	Argonne National Laboratory
ATW	Accelerator Transmutation of Waste
BOC	Beginning Of Cycle
B_4C	boron carbide
CS	Central Solenoid
EOC	End Of Cycle
FPD	Full Power Day
FPY	Full Power Year
FW	Fast Wave
FTWR-SC	Superconducting Fusion Transmutation of Waste Reactor
HT-9	a ferritic steel alloy
ICRF	Ion Cyclotron Range of Frequency
JET	Joint European Torus
k_{eff}	effective neutron multiplication constant of a fissioning assembly
LBE	Lead-Bismuth Eutectic
Li17Pb83	Lithium-lead eutectic 17 parts Li and 83 parts Pb
LWR	Light Water Reactor
MHD	Magneto-HydroDynamics
MT	Metric Tonne
MTU	Metric Tonne of initial Uranium
Nb_3Sn	Niobium Tin

NbTi	Niobium Titanium
OTC	Once-Through fuel Cycle
POPCON	Plasma Operating CONtour
Q_e	electric power amplification factor (electric power produced/electric power consumed)
Q_p	plasma energy amplification factor (fusion power/external heating power)
SNF	Spent Nuclear Fuel
TF	Toroidal Field
TRU	Trans-Uranics
W	Tungsten
ZrH	Zirconium Hidride

REFERENCES

1. "First Phase P&T Systems Study: Status and Assessment Report on Actinide and Fission Product Partitioning and Transmutation", OECD/NEA, Paris (1999).

2. "Proc. 1st-5th NEA International Exchange Meetings", OECD/NEA, Paris (1990,92,94,96,98).

3. "Nuclear Wastes--Technologies for Separations and Transmutations", National Research Council, National Academy Press, Washington (1996).

4. C. D. Bowman, et al., "Nuclear Energy Generation and Waste Transmutation Using Accelerator-Driven Intense Thermal Neutron Source", *Nucl. Instr. Methods, **A320***, 336 (1992).

5. W. C. Sailor, et al., "Comparison of Accelerator-Based with Reactor-Based Nuclear Waste Transmutation Schemes", *Progress in Nuclear Energy, **28***, 359 (1994).

6. "A Roadmap for Developing Accelerator Transmutation of Waste (ATW) Technology", US Dept. Energy report DOE/RW-0519 (1999).

7. T. A. Parish and J. W. Davidson, "Reduction in the Toxicity of Fission Product Wastes through Transmutation with Deuterium-Tritium Fusion Neutrons", *Nuclear Technology, **47***, 324 (1980).

8. E. T. Cheng, et al., "Actinide Transmutation with Small Tokamak Fusion Reactors", *Proc. Int. Conf. Evaluation of Emerging Nuclear Fuel Cycle Systems*, Versailles, France (1995).

9. Y-K. M. Peng and E. T. Cheng, "Magnetic Fusion Driven Transmutation of Nuclear Waste (FTW)", *J. Fusion Energy, **12***, 381 (1993).

10. E. T. Cheng and R. J. Cerbone, "Prospect of Nuclear Waste Transmutation and Power Production in Fusion Reactors", *Fusion Technology, **30***, 1654 (1996).

11. Y. Gohar, "Fusion Option to Dispose of Spent Nuclear Fuel and Transuranic Elements", Argonne National Laboratory report ANL/TD/TM00-09 (2000).

12. L. J. Qiu, Y. C. Wu, B. J. Xiao, et al., "A Low Aspect Ratio Tokamak Transmutation System", *Nuclear Fusion, **40***, 629 (2000).

13. W. M. Stacey, "Capabilities of a DT Tokamak Fusion Neutron Source for Driving a Spent Nuclear Fuel Transmutation Reactor", *Nucl. Fusion,* ***41***, 135 (2001).

14. W.M. Stacey, et al., "A Fusion Transmutation of Waste Reactor", Fusion Sci. Technol., 41, 116 (2002).

15. E.A. Hoffman, "Neutron Transmutation of Nuclear Waste," July 2002, Georgia Institute of Technology, Ph.D. Dissertation.

16. E.A. Hoffman and W.M. Stacey, "Nuclear Design and Safety Analysis for a Fusion Transmutation of Waste Reactor". Fusion Science & Technology, submitted (2002).

17. E.A. Hoffman and W.M. Stacey, "Comparative Fuel Cycle Analysis of Critical and Sub-critical Fast Reactor Transmutation Systems", Nuclear Technology, submitted (2002).

18. W. S. Yang and H. Khalil, "ATW System Point Design Employing LBE Cooled Blanket Design", Argonne National Laboratory Report (2000).

19. C.T. Jong, N. Mitchell and S. Sborchia, "The ITER-FEAT toroidal field structures," Fus. Eng. & Design 58-59 (2001) 165.

20. M. Huguet, "Key engineering features of the ITER-FEAT magnet system and implications for the R&D programme," Nucl. Fusion 41 (2001) 1503.

21. W.M. Stacey, "Capabilities of a DT Tokamak Fusion Neutron Source for Driving a Spent Nuclear Fuel Transmutation Reactor", Nucl. Fusion, 41, 135 (2001).

22. Los Alamos National Laboratory, http://www-xdiv.lanl.gov/XTM/dant/la12969/dantsys.html .

23. Los Alamos National Laboratory, http://laws.lanl.gov/x5/MCNP/index.html .

24. E.T. Cheng, C.W Maynard, W.F. Vogelsang and A.C. Klein, "Nucleonic Design for a Compact Tokamak Fusion Reactor Blanket and Shield," Wisconsin Fusion Design Memos, UWFDM-256, (1978).

25. J. Mandrekas, personal communication, Georgia Institute of Technology, Fusion Research Center, 2002.

26. ITER Team, "ITER Physics Basis," *Nucl. Fusion,* ***39***, 2137 (1999).

27. D.E. Post, N.A. Uckan, *Fusion Technology,* ***21***, 1427 (1992).

28. Y. Shimomura, et al., *Nucl. Fusion, **41***, 309 (2001).

29. T.S. Taylor, *Plasma Phys. Control. Fusion, **39***, B47 (1997).

30. T.K. Mau, personal communication, UCSD, April 2001.

31. S.C. Jardin, et al., *Fusion Eng. & Design, **38***, 27 (1997).

32. F. Engelmann, "Steady-State Operation of Magnetic Fusion Devices", *Nucl. Fusion, **40***, 1025 (2000).

33. University of California, Los Angeles Institute of Plasma and Fusion Research, "The ARIES-I Tokamak Reactor Study", Final Report, Volume I, UCLA-PPG-1323, 1 (1991).

34. M.R. Shay, et al., "Life-Cycle Cost Analysis for Developing and Deploying a Representative Accelerator Transmutation of Waste System," Pacific Northwest National Laboratory, PNNL-SA-32548, January 2000.

35. INTOR Phase 2A, Part III, Vol. 1, p. 444, International Atomic Energy Agency report STI/PUB-795, Vienna (1988).

36. International Nuclear Safety Center (http://www.insc.anl.gov/matprop/pbbi/pbbi.html) http://www.insc.anl.gov/matprop/pbbi/pbbiviscosity.pdf .

37. R.L. Klueh, Oak Ridge National Laboratory, personal communications, data from "Nuclear Systems Materials Handbook," Rev. 2.

38. ITER Technical Basis, Plant Description Document, G A0 FDR 1 01-07-13 R1.0.

39. ITER Physics, *ITER Documentation Series,* No. 21, IAEA, Vienna, 1991.

40. J. Wesson, *Tokamaks*, 2nd Edition, Oxford 1997.

41. R.J. Thome and J.M. Tarrh, *MHD and Fusion Magnets*, Wiley-Interscience, New York (1982).

42. W.M. Stacey, Jr., *Fusion*, Wiley Interscience, New York (1984).